THE EFFECT OF ADSORBED OXYGEN ON THE CONDUCTIVITY OF METAL-FREE PHTHALOCYANINE FILMS

A.E. Pochtennyi[1] & V.K. Dolgyi[2,*]

[1]*Belarusian State Technological University, 13A Sverdlov Str., Minsk, 220006, Belarus*

[2]*Belarusian State Agrarian Technical University, 99 Nezavisimost Ave., Minsk, 220023, Belarus*

*Address all correspondence to: Valeryi K. Dolgyi, Belarusian State Agrarian Technical University, 99 Nezavisimost Ave., Minsk, 220023, Belarus, E-mail: vsnaa@tut.by

The effect of adsorbed oxygen on the conductivity of vacuum-deposited metal-free phthalocyanine films was studied using the method of cyclic thermodesorption. The results are interpreted in terms of the two-level hopping conduction model. It is shown that the electron transport proceeds by hopping via combined system involving the intrinsic and impurity localized states.

KEY WORDS: *metal-free phthalocyanine, cyclic thermodesorption, hopping conduction, compensation effect, Meyer–Neldel rule*

1. INTRODUCTION

Phthalocyanine films are widely used in organic electronic devices such as gas sensors (Tomecek et al., 2018), solar cells (Wang et al., 2018), field-effect transistors (Yamada et al., 2018), and light-emitting diodes (Zhang et al., 2018). The operation of all these devices, based on the process of electron transport, is significantly influenced by oxygen adsorbed from the atmosphere. The insufficient knowledge about the mechanism of oxygen influence on the conductivity of phthalocyanine films hinders prediction and optimization of the properties of electronic devices employing these materials.

The purpose of this study was to elucidate the mechanism through which adsorbed oxygen influences the conductivity of metal-free phthalocyanine (H_2Pc) films and to determine contributions of the intrinsic and impurity centers of electron localization to the conductivity.

2. THEORETICAL AND EXPERIMENTAL DETAILS

The metal-free phthalocyanine films with a thickness of 200 nm were obtained by laser sputtering in a vacuum of 10^{-2} Pa, followed by precipitation of gaseous prod-

ucts of sputtering on polycore substrates equipped with an interdigital system of electrodes at room temperature. When this was made, a series of ten samples in a single vacuum cycle were obtained.

The surface structure was studied by employing atomic force microscopy with the use of a Solver PRO scanning probe microscope in a tapping mode. Atomic force microscopy showed that H_2Pc films are nanostructured ones.

The dc conductivity of PTCDI films was measured in a vacuum of 10^{-2} Pa with the aid of a V7E-42 electrometer. The investigation was performed by the method of cyclic thermodesorption (Pochtennyi and Misevich, 2003). According to this technique, a sample is heated to a certain preset temperature and then allowed to cool. In the course of cooling, the conductance of the sample G is measured as a function of the absolute temperature T and described in terms of the equation

$$G = G_0 \exp\left(-\frac{E_a}{kT}\right), \tag{1}$$

where G_0 is the preexponential factor, E_a is the conductivity activation energy, and k is the Boltzmann constant.

Variation of the oxygen concentration in the course of cooling was ignored because these measurements were performed in a vacuum.

The experiment consisted of a sequence of cycles, whereby the sample was heated to a stepwise increasing temperature T_0, which corresponded to a gradually decreasing concentration of adsorbed oxygen. By measuring the temperature variation of conductivity in the course of cooling the sample from this temperature in a vacuum, we obtained a family of curves corresponding to various concentrations of adsorbed oxygen on the same sample. Using this set of temperature dependences, we determined the corresponding room-temperature conductance G and the parameters G_0 and E_a corresponding to various concentrations of adsorbed oxygen. We used the cooling start temperatures T_0 of 40, 45, 50, 55, 60, 65, 70, and 75°C.

A complete set of data for all samples is shown in Fig. 1.

The data presented in Fig. 1 does not only indicate the presence of the compensation effect, the essence of which is that in a number of materials to large values of activation energy of conductivity there corresponds a higher value of the preexponential factor, but at the same time there is a linear relationship between these variables, which is consistent with the Meyer–Neldel rule (Meyer and Neldel, 1937) that takes into account measurement errors. The same conclusion can be reached on the basis of Fig. 2, showing how the data are consistent between different samples. The spread data from sample to sample are attributed to various adsorption capacities of different samples.

However, the situation is somewhat different when the data is not streamline patterns and not of the same temperature (see Figs. 3 and 4).
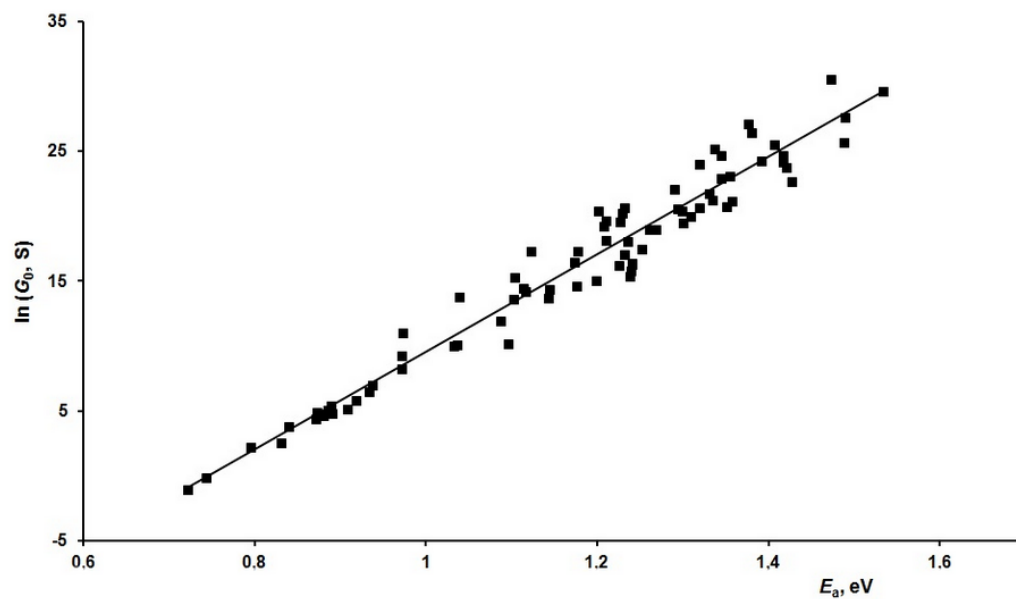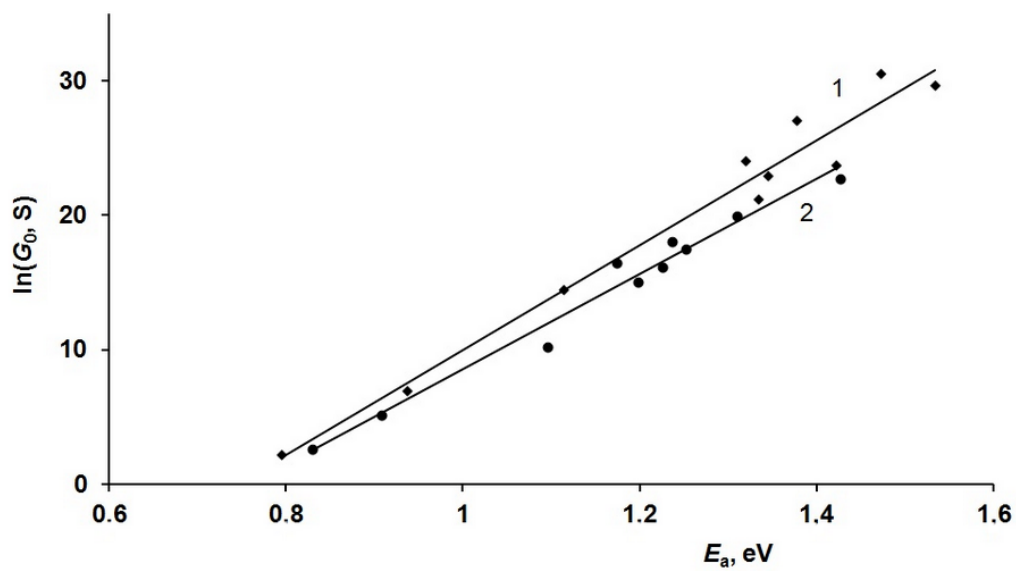
FIG. 1: Relation between the tunneling factor and conductivity activation energy for ten samples of metal-free phthalocyanine
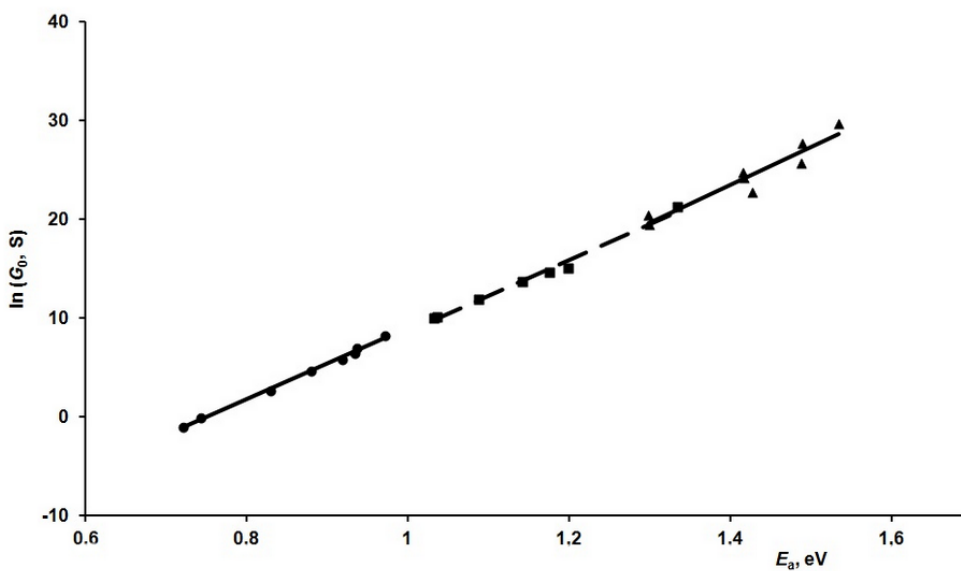
FIG. 2: Relation between the tunneling factor and conductivity activation energy for three samples of metal-free phthalocyanine
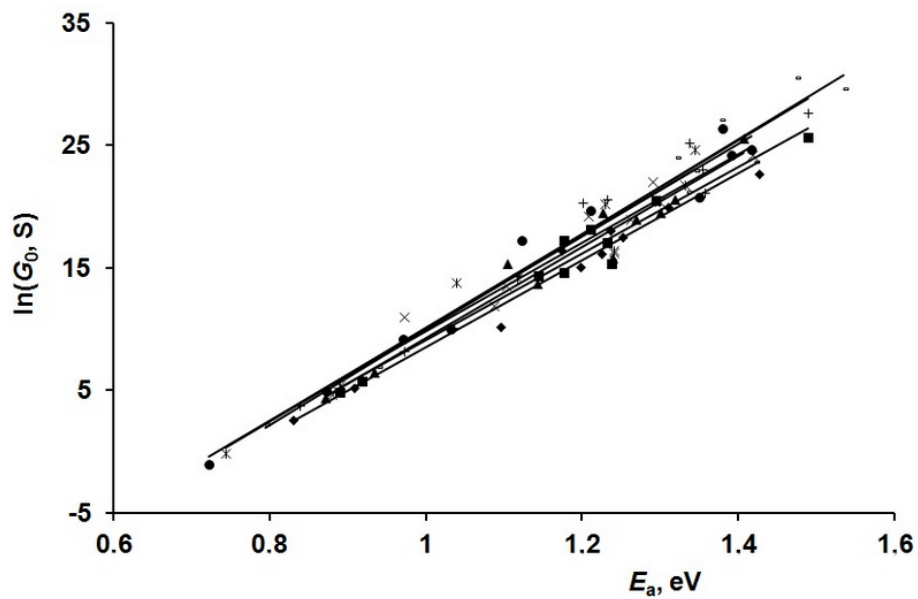
FIG. 3: Relation between the tunneling factor and conductivity activation energy at eight different temperatures

FIG. 4: Relation between the tunneling factor and conductivity activation energy at two different temperatures: 1) 40°C, 2) 75°C

Figures 3 and 4 show that the linear relations relating the tunneling factor and activation energy of conductivity have different slopes monotonically decreasing with increasing temperature.

To explain the observed fact, we use the model of a two-level hopping conduction (Pochtennyi and Misevich, 2003), according to which the electron transfer is carried out through two parallel channels — intrinsic and impurity electron states of localization with radii a_1 and a_2, respectively. In this case, the conductance is

$$G = (G_{03})_1 \exp\left(-\frac{\alpha}{a_1 n_1^{1/3}} - \frac{E_{a1}}{kT}\right) + (G_{03})_2 \exp\left(-\frac{\alpha}{a_2\, n_2^{1/3}} - \frac{E_{a2}}{kT}\right), \qquad (2)$$

where $(G_{03})_1$ and $(G_{03})_2$ are constants depending on the localization radius, $\alpha = 1.73$ is the percolation constant, n_1 and n_2 are the concentrations of localization centers corresponding to the intrinsic and impurity states, and E_{a1} and E_{a2} are the conductivity energies of activation of intrinsic and impurity states, respectively.

The quantities E_{a1} and E_{a2} are defined by the relations

$$E_{a1} = \frac{0.99e^2\, n_1^{1/3}}{4\pi\varepsilon_0\varepsilon}, \quad E_{a2} = \frac{0.99e^2\, n_2^{1/3}}{4\pi\varepsilon_0\varepsilon}, \qquad (3)$$

where ε_0 is the electric constant and ε is the relative permittivity.

Since the impurity levels are formed due to the splitting-off from the intrinsic levels, the concentration of electron localization centers of intrinsic and impurity states are connected by the relation

$$n_1 + n_2 = n = \text{const}. \qquad (4)$$

In this case, the temperature dependence of the conductivity is described by relation (1) and the experimentally observable conductivity activation energy appearing in this relation and the quantity of the tunneling factor are calculated as

$$E_a = -\frac{d(\ln\sigma)}{d(1/kT)}, \quad G_0 = G\exp\left(\frac{E_a}{kT}\right). \qquad (5)$$

The result of calculation of the two-level model of hopping conduction is shown in Fig. 5. In the calculations, $a_1 = 4.25\cdot10^{-10}$ m, $a_2 = 2.7\cdot10^{-10}$ m, and $n = 1.69\cdot10^{27}$ m^{-3}.

Figure 5 shows the relation of the tunnel factor with conductivity activation energy, calculated by a two-level model of hopping conduction, corresponding to the so-called compensation effect on all sectors of the curve.

AB and *BC* areas have been observed previously for led phthalocyanine (Pochtennyi and Misevich, 2003) and for perylene pigment (Pochtennyi and Lappo, 2005).
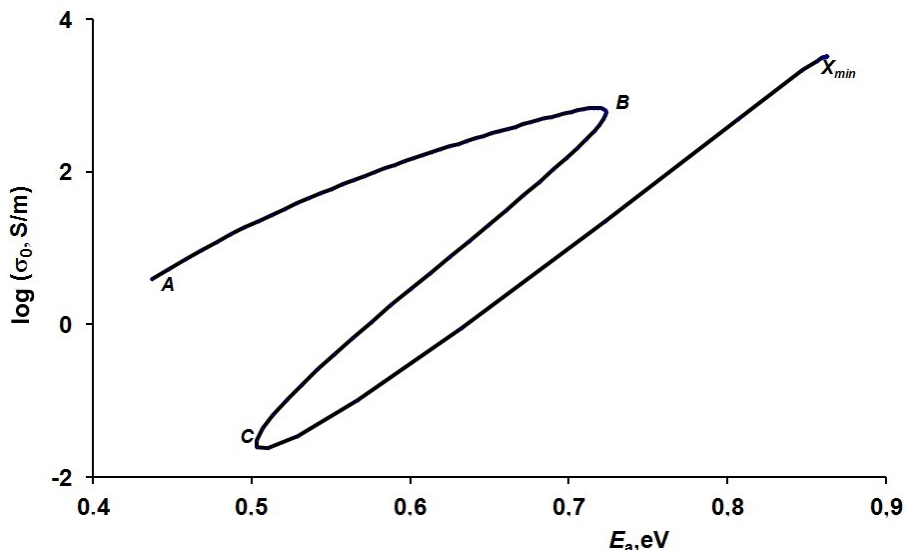
FIG. 5: Relation between the tunneling factor and conductivity activation energy, calculated from the two-level model of hopping conduction

The minimum concentration of the sorbed oxygen in the films allows H_2Pc count on getting CX_{min} portion of the curve in Fig. 5.

Corresponding calculations for low impurity concentrations are shown in Figs. 6–9. Figures 6 and 7 show that within the area CX_{min} the conductivity activation energy and the tunneling factor are due to both the intrinsic and impurity states. Figure 8 also shows that in this concentration range there is a transition from intrinsic to the impurity conductivity, and Fig. 9 shows that in this range of impurity concentrations the tunneling factor is many orders of magnitude greater than the conductivity value, i.e., in terms of

$$\ln (G_0) = \ln G + \frac{E_a}{kT}, \tag{6}$$

the $\ln G$ value is negligibly small in comparison with other terms.

In this case, the slope of the line between the tunneling factor and conductivity activation energy must be equal to $1/kT$. In other words, if you build a graph of the experimental value of the above tangent $1/kT$, you should get a straight line having a slope of one. This dependence is shown in Fig. 10 and has a slope of 0.943, which, taking into account measurement errors, is really close to the intended value.

Theoretical modeling using formulas (1)–(5) allows one to compare the experimental data obtained for metal-free phthalocyanine films with the calculated results. This comparison is made in Fig. 11 and shows good agreement between the theoretical and experimental data.
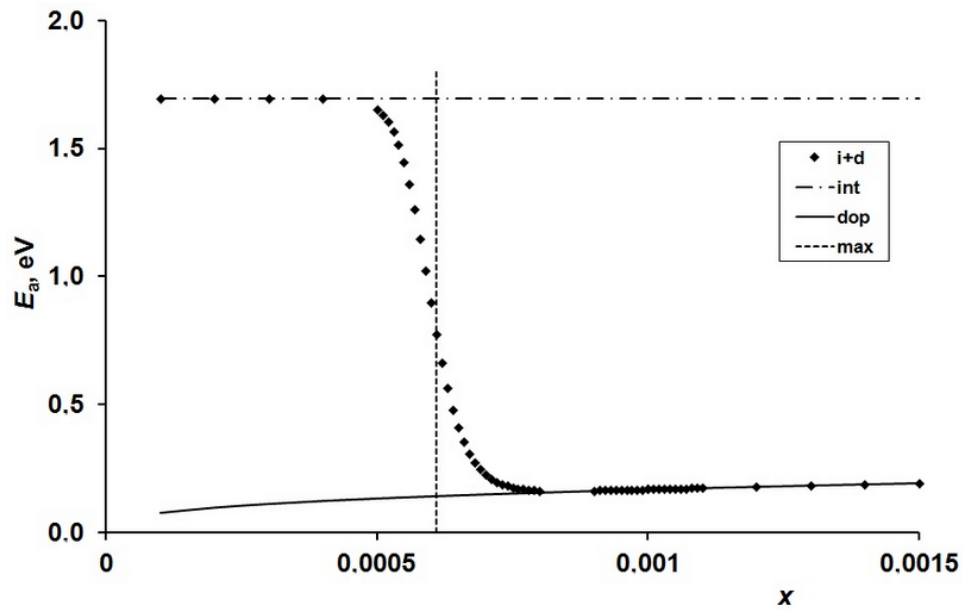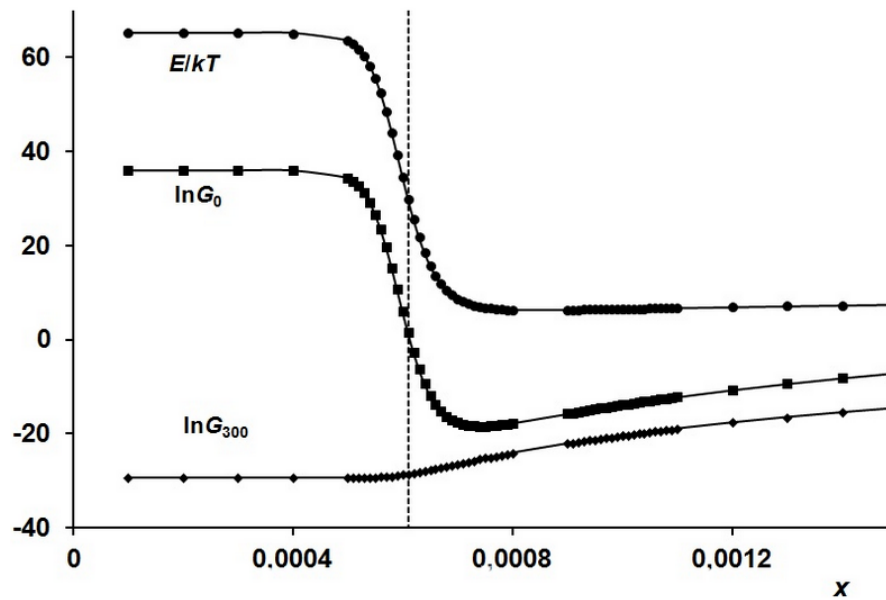
FIG. 6: Theoretical dependence of conductivity activation energy on the relative concentration of impurities at low concentrations
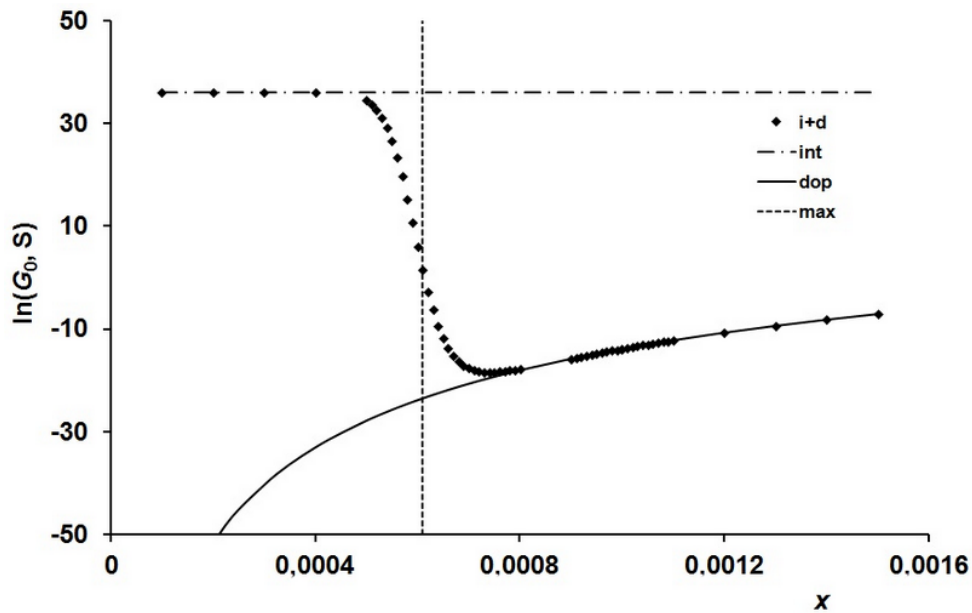
FIG. 7: Theoretical dependence of the tunneling factor on the relative concentration of impurities at low concentrations
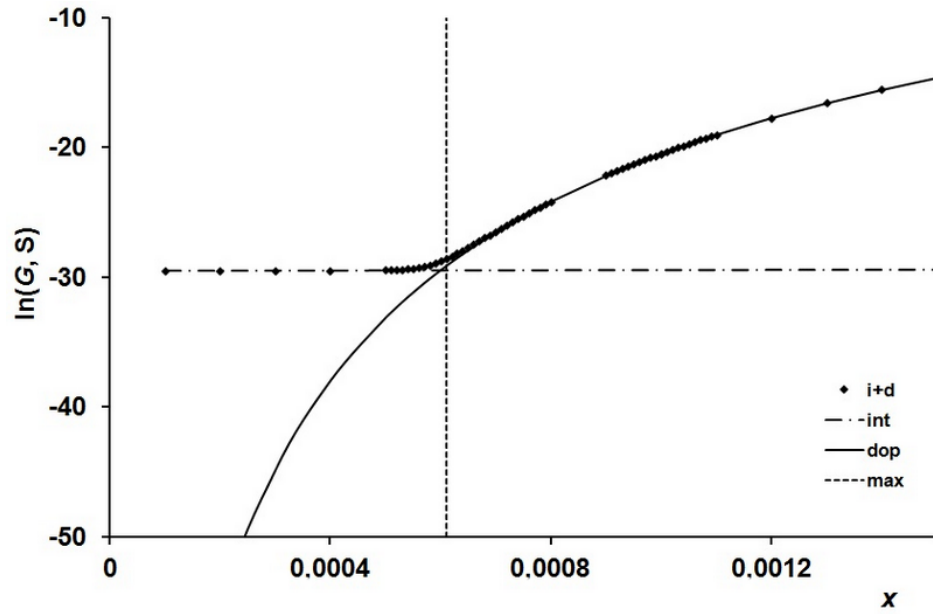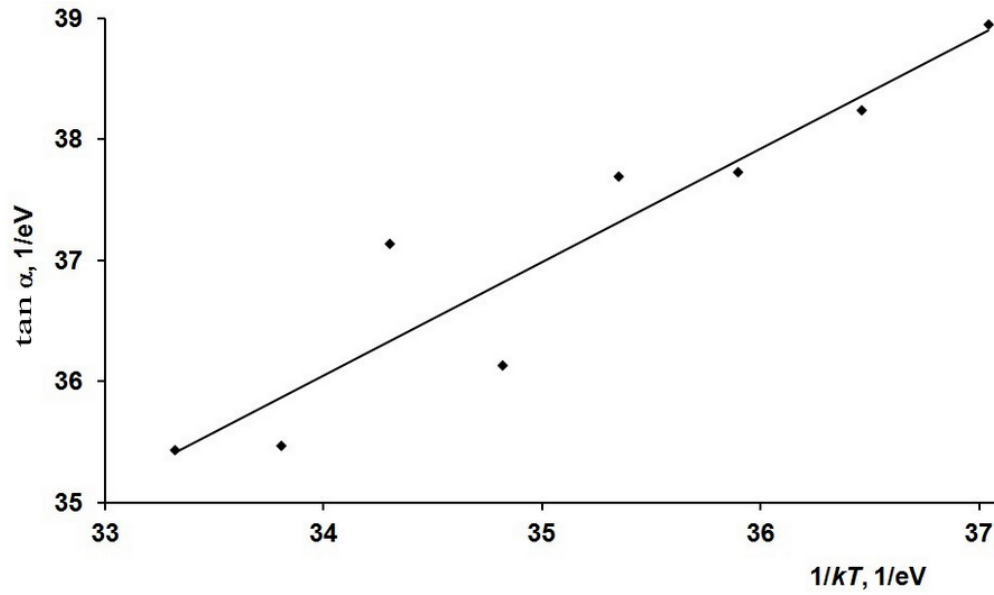
FIG. 8: Theoretical dependence of conductivity on the relative concentration of impurities at low concentrations
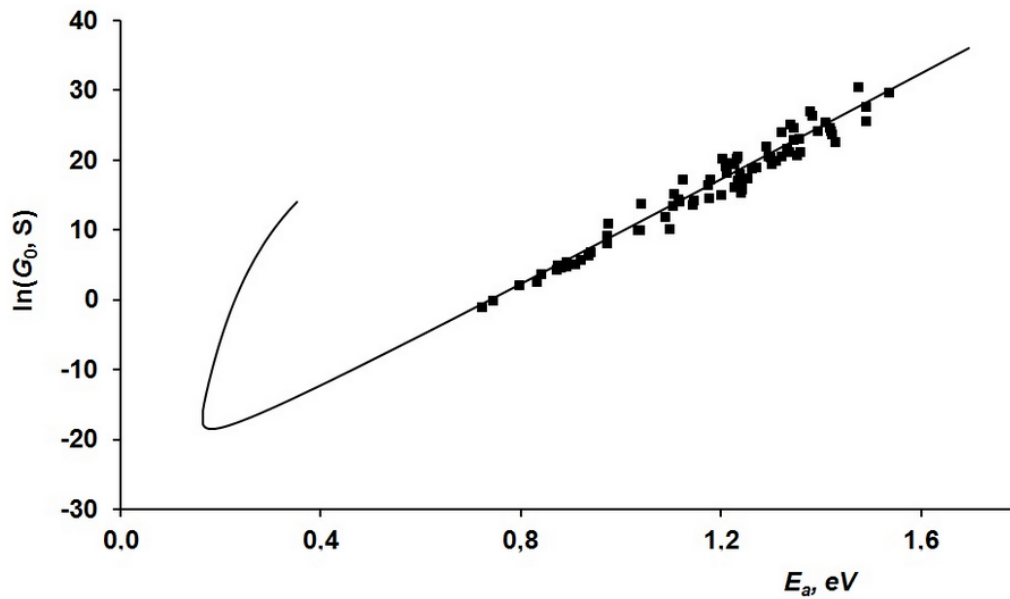

FIG. 9: Joint theoretical dependence of conductivity activation energy, tunneling factor, and conductivity on the relative concentration of impurities at low concentrations

FIG. 10: Relation between the experimental and theoretical values of the slope of dependence (6)

FIG. 11: Experimental (points) and theoretical (line) relations between the tunnel factor and conductivity activation energy of metal-free phthalocyanine films

3. CONCLUSIONS

Thus, by comparing the experimental data obtained using the method of cyclic thermodesorption with the results of calculations performed within the framework of a two-level hopping conduction model, we have evaluated the radii of electron localization in the intrinsic and impurity states and the concentration of the localization centers in metal-free phthalocyanine films. It was established that the conductivity of these films is provided by a combined system of intrinsic and impurity electron states.

REFERENCES

Meyer, W. and Neldel, H., A Relation between the Energy Constant ε and the Quantity Constant α in the Conductivity–Temperature Formula for Oxide, *Z. Tech. Phys.*, vol. **18**, pp. 588–593, 1937.

Pochtennyi, A.E. and Lappo, A.N., The Effect of Adsorbed Oxygen on the Conductivity of Perylenetetracarboxylic Acid *N,N*-Dimethyldiimide Films, *Tech. Phys. Lett.*, vol. **31**, no. 2, pp. 34–40, 2005.

Pochtennyi, A.E. and Misevich, A.V., The Effect of Adsorbed Oxygen on the Conductivity of Lead Phthalocyanine Films, *Tech. Phys. Lett.*, vol. **29**, no. 1, pp. 56–61, 2003.

Tomecek, D., Fitl, P., Vlcek, J., Maresova, E., and Vrnata, M., Detection of Taggants in Explosives on Nanostructured Metal/Silver Phthalocyanine Chemiresistors: Influence of Analyte Photoactivation, *Sensors Actuators B: Chem.*, vol. **239**, pp. 147–156, 2018.

Wang, Y., Shan, H., Sun, X., Dong, L., and Xu, Z., Fabrication of Octamethyl Substituted Zinc(II) Phthalocyanine Nanostructure via Exfoliation and Use for Solution-Processed Field-Effect Transistor, *Organic Electronics*, vol. **55**, pp. 15–20, 2018.

Yamada, K., Yoshimi, S., Katagiri, C., and Nakayama, K., High Vertical Carrier Mobility in the Nanofiber Films of a Phthalocyanine Derivative and Its Application to Vertical-Type Transistors, *Organic Electronics*, vol. **53**, pp. 320–354, 2018.

Zhang, X., Zhang, M., Liu, M., Chen, Y., and Huang W., Highly Efficient Tandem Organic Light-Emitting Devices Adopting a Nondoped Charge-Generation Unit and Ultrathin Emitting Layers, *Organic Electronics*, vol. **53**, pp. 353–360, 2018.